The American Journal of Human Genetics, Volume *103*

Supplemental Data

DNA Polymerase Epsilon Deficiency Causes

IMAGe Syndrome with Variable Immunodeficiency

Clare V. Logan, Jennie E. Murray, David A. Parry, Andrea Robertson, Roberto Bellelli, Žygimantė Tarnauskaitė, Rachel Challis, Louise Cleal, Valerie Borel, Adeline Fluteau, Javier Santoyo-Lopez, SGP Consortium, Tim Aitman, Inês Barroso, Donald Basel, Louise S. Bicknell, Himanshu Goel, Hao Hu, Chad Huff, Michele Hutchison, Caroline Joyce, Rachel Knox, Amy E. Lacroix, Sylvie Langlois, Shawn McCandless, Julie McCarrier, Kay A. Metcalfe, Rose Morrissey, Nuala Murphy, Irène Netchine, Susan M. O'Connell, Ann Haskins Olney, Nandina Paria, Jill A. Rosenfeld, Mark Sherlock, Erin Syverson, Perrin C. White, Carol Wise, Yao Yu, Margaret Zacharin, Indraneel Banerjee, Martin Reijns, Michael B. Bober, Robert K. Semple, Simon J. Boulton, Jonathan J. Rios, and Andrew P. Jackson

Supplemental Note: Case Reports

Skeletal Features: Metaphyseal dysplasia was a defining feature of the original IMAGe association[1]. In these initial case reports, the metaphyses were reported to be striated and irregular. Osteopenia, delayed bone age and small epiphyses were also noted. With the identification of *CDKN1C* mutations as a cause of IMAGe syndrome, it became evident that metaphyseal changes and the other skeletal findings were variably present and could be expanded to include scoliosis[2]. The identified skeletal abnormalities are age-dependent, can be absent or subtle[3] and most commonly manifest as delayed bone age and short stature[3]. Similar skeletal involvement is seen in *POLE* deficient IMAGe subjects, with generalised undermineralisation (osteopenia) and bilateral hip dysplasia being the most commonly reported (n=8). Metaphyseal widening and striations were previously reported in P13[4] and P12[5]. P1 and P6 also have metaphyseal involvement characterized by a sclerotic metaphyseal band and mild widening. Scoliosis (n=3), increased epiphyseal density in distal phalanges (n=1), 11 rib pairs (n=2), absent/hypoplastic patella (n=2), brachydactyly (n=1) were reported in other cases. P4 had no clear metaphyseal abnormalities (though growth plates were closed in this adult patient, age 50), however osteopenia and an increased upper thoracic kyphosis were present. Metaphyseal striations were also reported with the previously reported c.4444+3A>G mutation (which was denoted, 'FILS syndrome', mild facial dysmorphism, immunodeficiency, livedo, and short stature)[6].

Habitus: In the three adult subjects (P1, 4, 10), central adiposity and thin extremities were noted.

Neurocognition: Developmental delay/learning disability varied from normal or mild speech delay to moderate-severe impairment. Three individuals developed seizures with at least two occurring in childhood. MRI neuroimaging, normal (n=3), pituitary hypoplasia (P7, P13, P15), hypoplastic corpus callosum with small flattened pituitary and ventriculomegaly (P5); prominent extra-axial CSF with some periventricular high signal in frontal lobes (P1).

Infancy: Many families reported feeding difficulties as neonates, with six subjects progressing to gastrostomy insertion. Early respiratory problems were also noted included tracheomalacia and respiratory distress requiring CPAP support. Hypoglycaemia was also reported.

Malformations: Malformations were uncommon: atrial septal defect (P7), and unilateral hydronephrosis with proximal hydroureter (P3).

Supplemental Figures

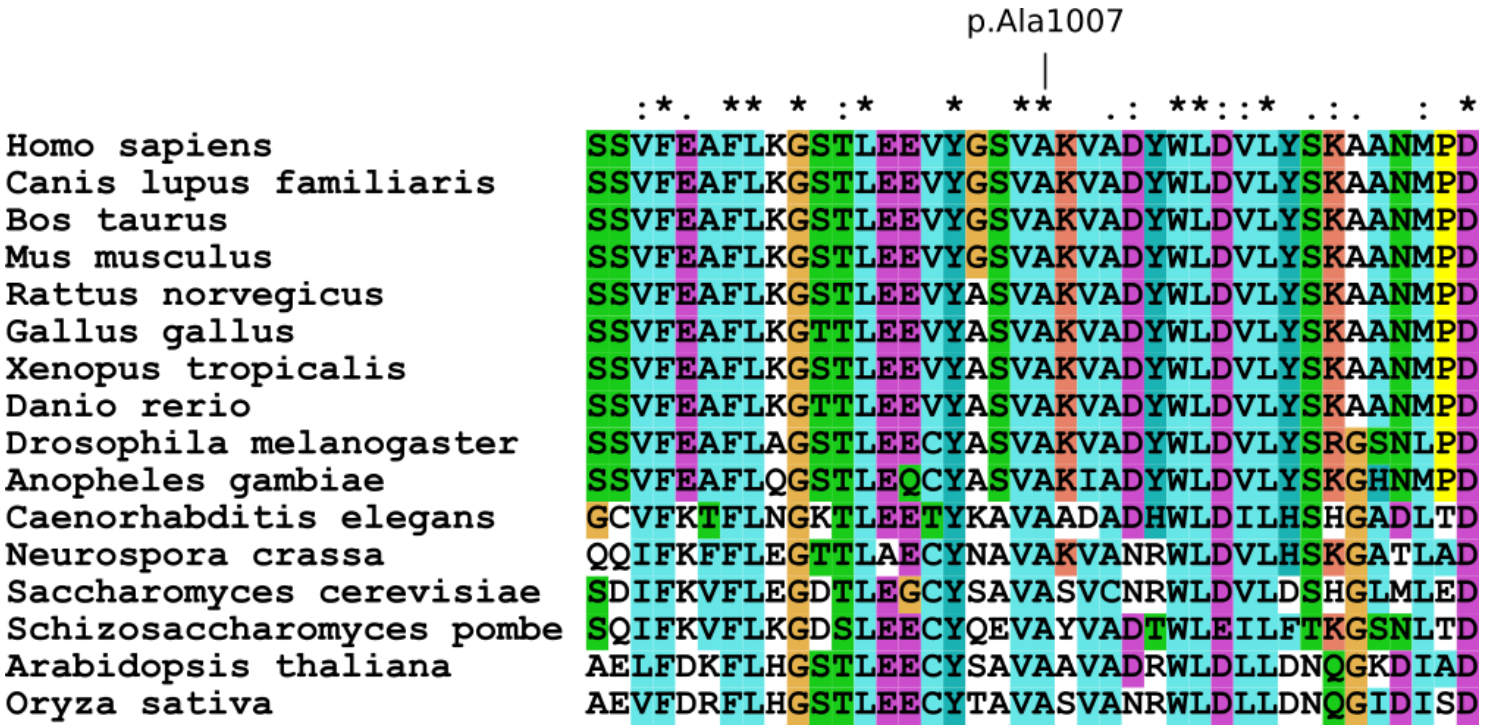

Figure S1: ClustalX alignment of POLE1 orthologs showing human p.Ala1007 and flanking residues.
The position of human alanine 1007 (mutated to proline in patient P10) is marked above the alignment. Asterisks indicate fully conserved positions, colons indicate positions with conservation between groups of strongly similar properties (PAM250 score > 0.5) and dots indicate conservation between groups with weakly similar properties (PAM250 score ≤ 0.5). Protein accessions used: Homo sapiens, NP_006222.2; Canis lupus familiaris, XP_543348.3; Bos taurus, NP_001178358.1; Mus musculus, NP_035262.2; Rattus norvegicus, NP_001100622.2; Gallus gallus, XP_004934482.1 ; Xenopus tropicalis, XP_004910692.1; Danio rerio, NP_001121995.1; Drosophila melanogaster, NP_524462.2; Anopheles gambiae, XP_315205.4; Caenorhabditis elegans, NP_493616.1; Neurospora crassa, XP_955939.2; Saccharomyces cerevisiae, NP_014137.1; Schizosaccharomyces pombe, NP_596354.1; Arabidopsis thaliana, NP_172303.5; Oryza sativa, NP_001046939.2.

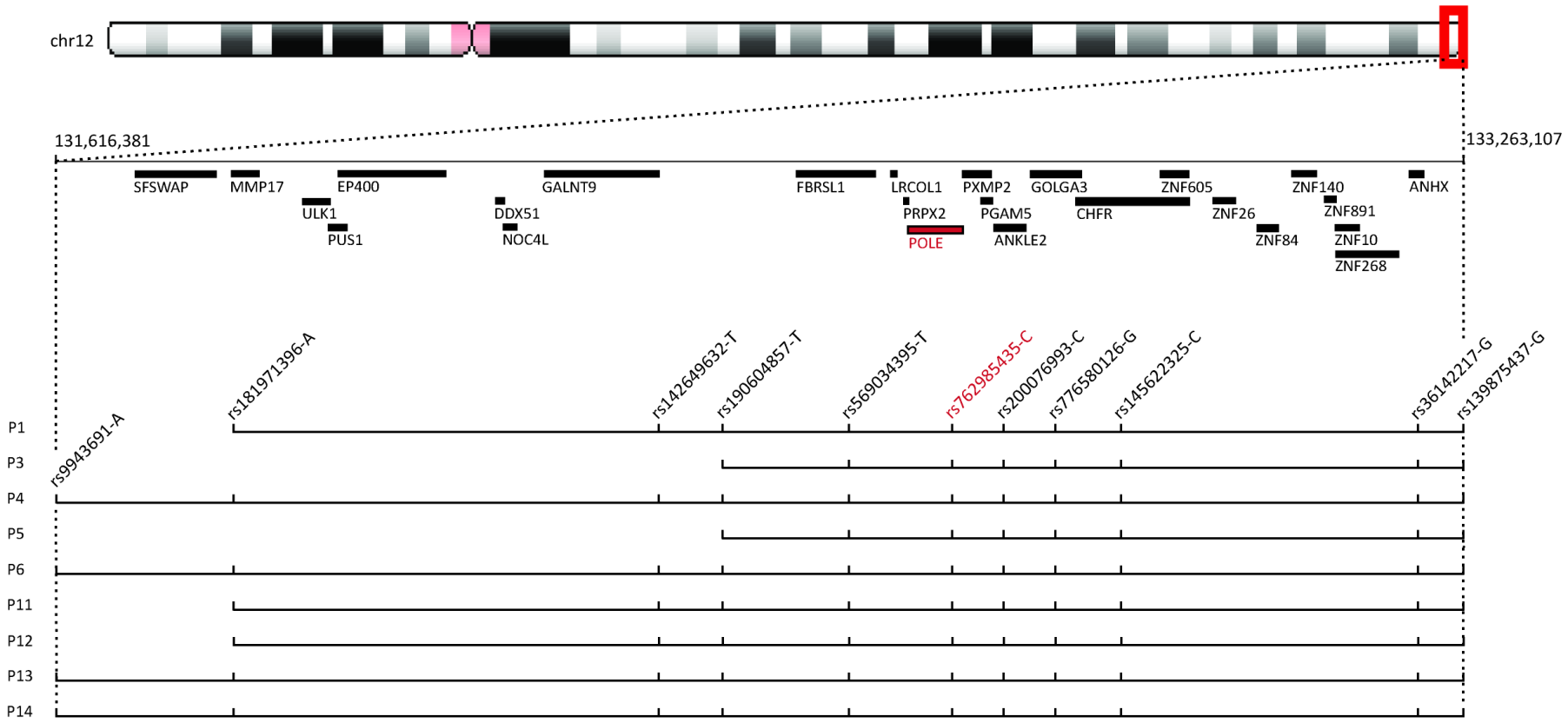

Figure S2: Schematic of region of chromosome 12q24.33, depicting shared haplotype region.
rs762985435 (red), c.1686+32C>G *POLE.* dbSNP identifiers and the allele present on the shared haplotype provided. Lines indicate the extent of the shared haplotype for different subjects.

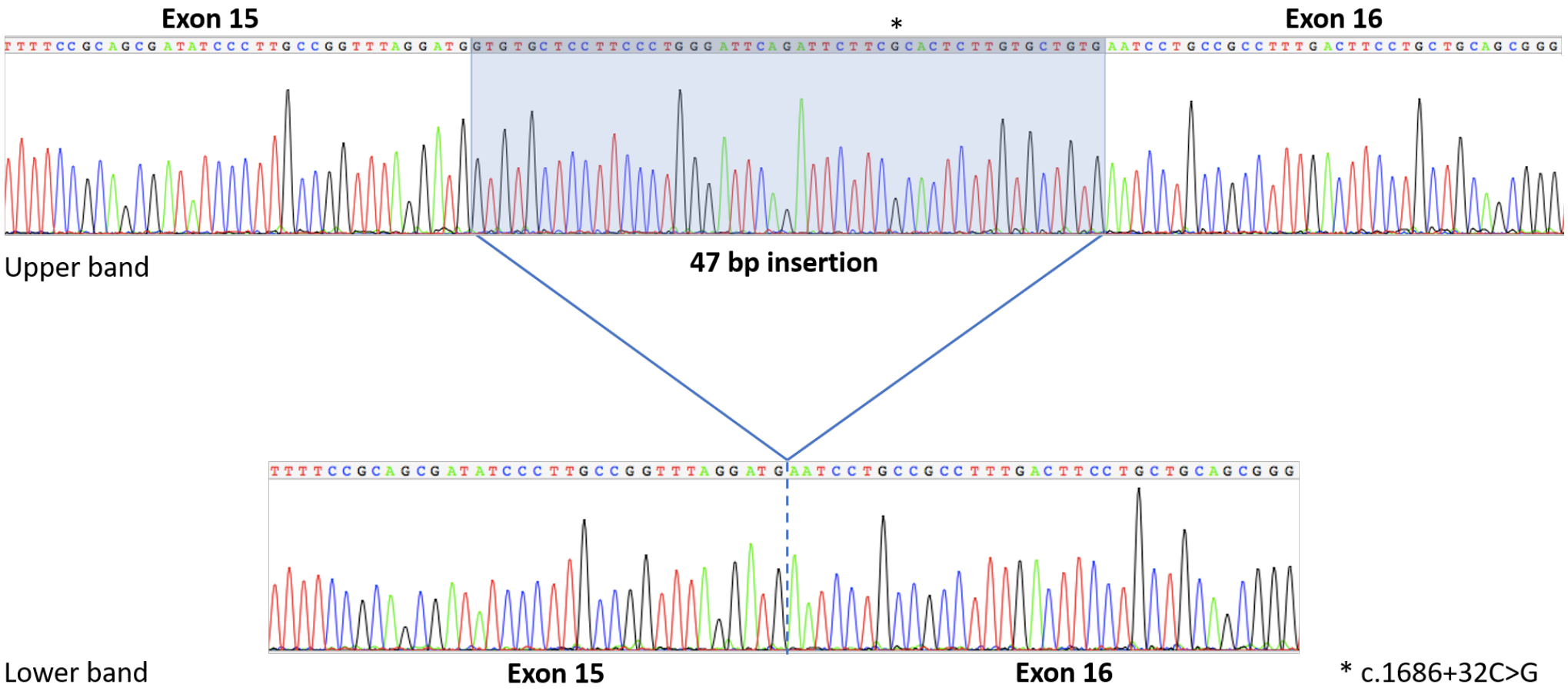

Figure S3: Representative Sanger sequencing electropherograms of POLE transcripts from P1.
POLE cDNA amplified with primers as indicated in Fig 3A, with sequence corresponding to upper and lower bands in this figure panel. The upper band includes 47 bp of intron 15 (highlighted in blue). The c.1686+32C>G variant is evident in the retained intronic sequence, indicated by asterix.

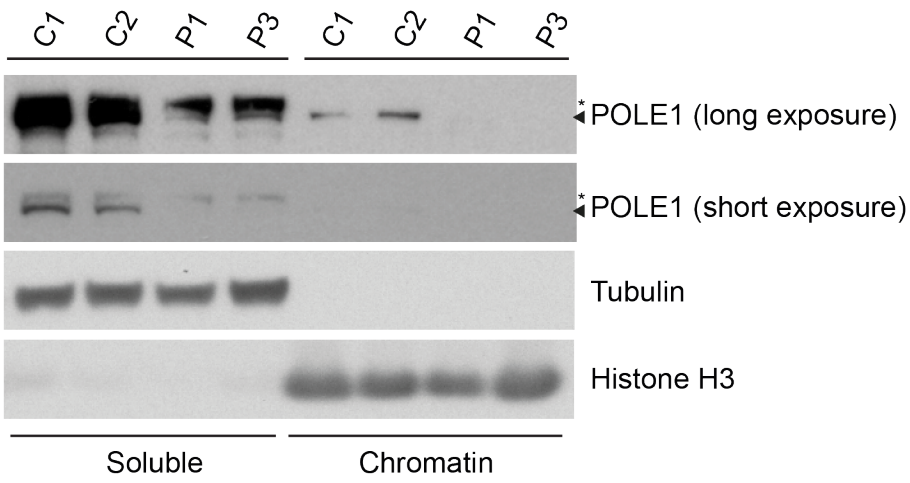

Figure S4. Chromatin Fractionation and Immunoblotting of POLE1
Western blot analysis of POLE1 from total soluble and chromatin fractions of control (C1, C2) and patient derived (P1, P3) primary fibroblasts lines. Antibody (GTX132100) raised against recombinant protein encompassing a sequence within the N-terminus region of human POLE1. Tubulin and Histone H3, loading controls respectively for soluble and chromatin-associated proteins. * denotes, non-specific band. Short exposure, ~30s; long exposure, ~20mins.

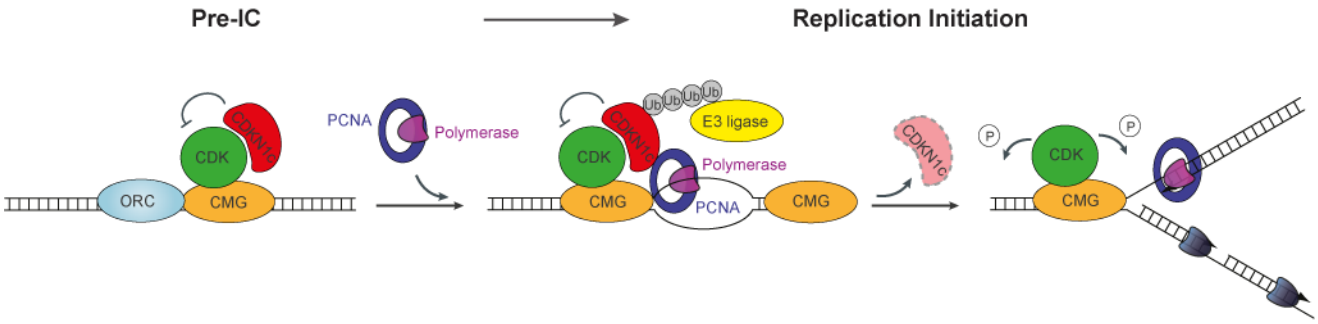

Figure S5. Hypothetical model of functional relationship between CDKN1C and PCNA/DNA polymerase loading.

Mutations in POLE1 and CDKN1C both cause IMAGe syndrome, suggesting a potential functional relationship. PCNA is required for CDKN1C ubiquitination[2], and overexpression experiments have established that CDKN1C-IMAGe mutations both disrupt PCNA binding[2] and result in increased protein stability[7; 8]. However the context, cell-cycle timing and location for PCNA binding and CDKN1C degradation has not yet been established. Biochemical studies on Xenopus CDKN homologs using egg extracts suggest that CDKNs may inhibit CDK activity, until PCNA/polymerase loading onto DNA triggers their ubiquitination and proteolytic degradation during replication fork initiation[9; 10]. The relevance of these findings to somatic mammalian cells and CDKN1C remain to be determined. CDK, Cyclin dependent kinase; ORC, Origin Recognition Complex; CMG complex (CDC45, MCM2-7, GINS); Ub, ubiquitin; P, phosphorylation of target proteins by CDK.

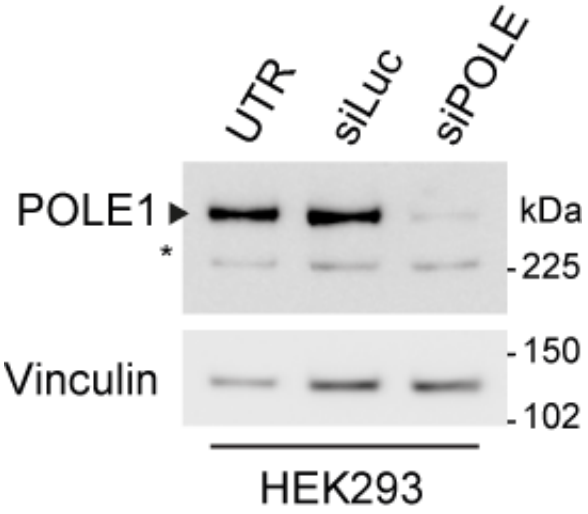

Figure S6. **Validation of POLE1 monoclonal antibody (93H3A)**.
The antibody used (93H3A) was raised against recombinant human POLE1 corresponding to aa1-176. UTR, untransfected. siLuc, negative siRNA control. siPOLE, siRNA targeting *POLE* transcript. *, non-specific band. Vinculin was used as a loading control.

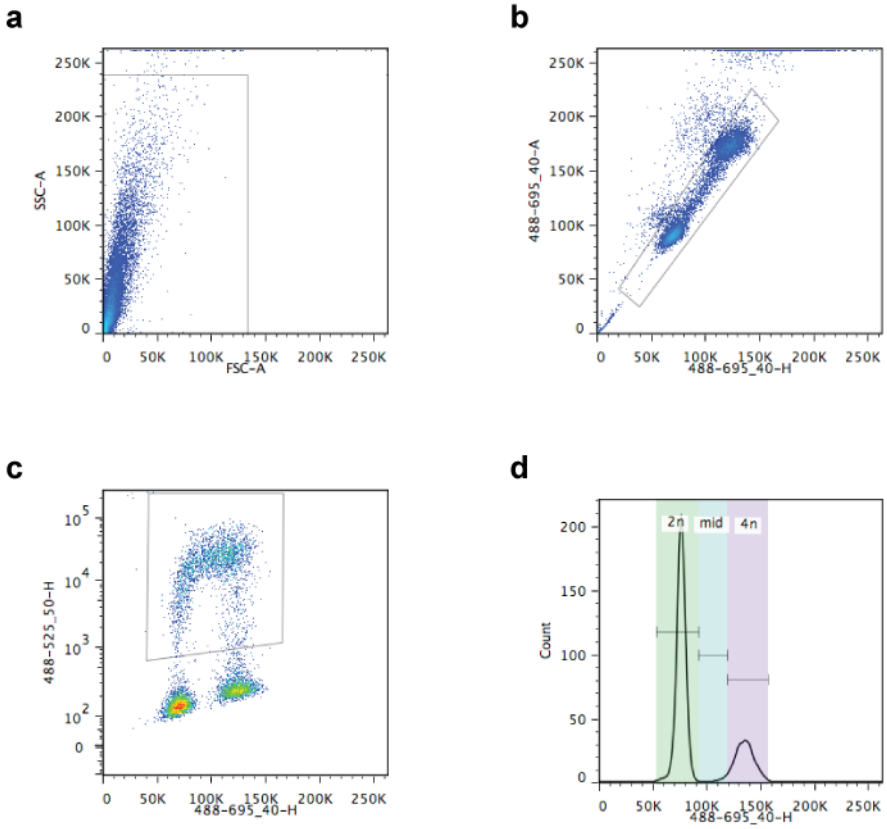

Figure S7. Gating strategy for FACS-cell cycle analysis, for experiment depicted in Fig 3c,d. Cells gated on FSC/SSC as indicated (**a**), and doublet cells then removed (**b**). BrdU-labelled population then gated (**c**), and 2n, 4n and mid-S phase populations defined (**d**). Representative plots for C1, 0 h time point (a-c), except bottom right (d) C1, 8 h time point shown, as 2n, 4n populations are most distinct at this time point

Supplemental Tables

	Primordial dwarfism	**gnomAD All Populations**
LoF	3	198
No LoF	93	277078
***P*-Value**	5.10×10^{-5}	

Table S1. *POLE* Allele counts. Whole-genome sequenced subjects from Primordial dwarfism cohort (n=48) versus gnomAD database (n=138,638, WGS/WES). *P*-value, one-tailed Fisher's exact test. LoF, loss of function.

ID	Prenatal Growth				Postnatal growth			
	Gest^{n} /wks	Weight /kg (s.d.)	Length /cm (s.d.)	OFC /cm (s.d.)	Age at exam	Weight /kg (s.d.)	Height /cm (s.d.)	OFC /cm (s.d.)
P1	31	0.926 (-2.8)	35* (-5.8)	26.6 (-2.0)	18yrs	18.25 (-14)	109.9 (-9.6)	48.5 (-5.1)
P3	41	2.5 (-2.6)	n/a	34.8 (-0.8)	7yrs	15 (-3.9)	93.8 (-5.5)	49.4 (-2.7)
P4	40+6	2.49 (-2.4)	n/a	n/a	50yrs	n/a	88 (-12.5)	46 (-8.03)
P5	39	2.4 (-2.1)	42.5 (-3.9)	34 (-0.5)	11yrs 7mths	14.3 (-8.6)	99.2 (-6.8)	47.4 (-4.7)
P6	35	1.42 (-2.8)	40 (-3.5)	28 (-2.8)	9yrs 6mths	15 (-5.3)	100.7 (-5.7)	46.7 (-5.5)
P7	38	2.1 (-2.4)	41.9 (-3.8)	n/a	13yrs	20.1 (-5.3)	106.1 (-6.2)	47 (-5.2)
P8	34	1.3 (-2.8)	n/a	n/a	2yrs 9mths	5 (-10.4)	66.6 (-7.5)	41 (-7.3)
P9	37	1.56 (-3.3)	n/a	n/a	1yr 7mths	4.4 (-9.3)	59.2 (-7.7)	42.5 (-4.7)
P10	40	1.45 (-4.9)	42 (-4.4)	32 (-2.1)	39yrs	13.8 (-16.8)	95.6 (-11.27)	n/a
P11	37	1.4 (-3.8)	39 (-4.8)	29 (-3.0)	-	n/a	n/a	n/a
P12	34	1.26 (-2.8)	38 (-4.2)	28 (-2.3)	12yrs	11 (-9.14)	113 (-5.07)	At 6 months 35.5 (-5.8)
P13	40	2.07 (-3.2)	42 (-4.5)	33 (-1.7)	-	n/a	n/a	n/a
P14	36	1.8 (-2.2)	44 (-1.7)	32.5 (-0.2)	18yrs 7mths	24.5 (-7.9)	112.7 (-8.4)	n/a
P15	40	1.35 (-3.9)	40 (-4.3)	30.5 (-2.2)	31yrs	16.8 (-15.6)	103 (-10.6)	'microcephaly'

Table S2: Anthropometric measurements in *POLE* individuals with biallelic mutations. ID, Individual number. Gest^{n}, gestation. wks, weeks. s.d., Z-scores calculated with LMS growth using British 1990 dataset. *measurement at age 3 weeks (first available postnatal measurement). P15 OFC measurement not available but documented to have microcephaly although OFC not as severe as height.

ID	Age	Endocrine			Genitourinary		Skin			
		Adrenal Insufficiency	Age at diagnosis	Additional Information	Hypospadias	Bilateral Cryptorchidism	Eczema	Café aux lait	Livedo	Additional Information
P1	18yrs	Y	18mths	Presented in adrenal crisis. Developed Insulin resistance, delayed puberty, fatty liver & hypertriglyceridaemia (likely related to stem cell transplant)	Y	Y (descended later in childhood)	Y	N	N	
P3	7yrs	Y	5yrs	Presented with hypoglycaemic episodes. No response to GH therapy	Y (mild)	Y (hypoplastic scrotum)	N	N	N	
P4	50yrs	N	-	Normal cortisol but dynamic testing not performed	Female	Female	Y	N	N	
P5	11yrs 7m	Y	7yrs	Neonatal hypothyroidism. Panhypopituitarism at 12 months including GH deficiency. Small, flattened pituitary on MRI.	Y	Y	N	N	N	
P6	9yrs 6m	Y	Neonate	Nephrocalcinosis & hypercalciuria at 6mths. GH deficiency.	Female	Female	N	N	Intermittent	Psoriasis from 11 yrs, Livedo improved with age
P7	13yrs	Y	Neonate	Low GH identified at 14mths, low ACTH at 22mths with low cortisol, hypothyroid at 3yrs	Y (ambiguous genitalia)	Y	Y	N	N	
P8	4yrs 2m	Y	4yrs	Hyponatraemia identified during prolonged viral infection. GH deficiency.	N	Y	N	N	N	
P9	2yrs 3m	N	-	Normal cortisol but dynamic testing not performed	Female	Female	N	N	N	
P10	39yrs	Y	Neonate	Pigmentation at birth. Presented with salt wasting crisis. GH deficiency but no response to GH therapy.	Female	Female	N	Y	N	
P11	3m	N	-	-	Female	Female	N	Y	N	
P12	12yrs	Y	Neonate	No response to GH therapy. Diabetes. Affected sister (P11) found to have small adrenal glands with abnormal cortex and small pituitary on post-mortem examination	Female	Female	N	N	N	

P13	8yrs	Y	4yrs 6mths	Progressive pigmentation at 4yrs. Small anterior pituitary on MRI. GH deficiency but no response to GH therapy.	Y	Y	N	Y	N	
P14	18yrs 7m	Y	4yrs	Hyponatraemic seizure at 4yrs. Hypercalcaemia in infancy. Normal cortisol at 6mths. Severe failure to thrive, chronic diarrhoea and pancreatic enzyme deficiency. GH deficiency with no response to GH therapy	Female	Female	N	Y	N	
P15	31yrs	Y	2yrs	Presented with hypoglycaemia & seizures at 2yrs. Pituitary hypoplasia on MRI.	N	Y	N	Y	N	

Table S3: Endocrine, Genitourinary, Immune and Skin findings in POLE deficient individuals. ID, Individual number. Growth Hormone (GH) deficiency established through provocative testing. P1, developed lactic acidosis during trial of metformin. Yrs, years; m, months.

ID	Clinically increased infection Y/N	Bacterial	Viral	Fungal	Neutro-phils X 10^9/L *(normal range)*	Lymphocyte Subsets				Immunoglobulins			Additional Information
						CD3+CD4+ X 10^6/L	**CD3+CD8+** X 10^6/L	**CD19** X 10^6/L	**NK cells** X 10^6/L	**IgG** g/L	**IgA** g/L	**IgM** g/L	
P1	Y	Pseudomonas aeruginosa, Klebsiella pneumoniae	CMV Severe EBV (required BMT)	Candida albicans	Normal 3-4.8 (1.5-8)	Normal 1040 (300-2000)	Normal 770 (300-1800)	Low <10 (200-1600)	Low 10 (90-900)	Normal 10.4 (7.68-17.28)	Normal-High 6.41 (0.77-1.67)	Low 0.28 (0.57-2.66)	EBV haemophagocytic lymphohistiocytosis requiring stem cell transplant. Severe local reactions to immunisations. Normal response to tetanus, moderate response to HiB, absent response to pneumococcus
P2	Y	N	HSV	N	n/a	n/a	n/a	n/a	n/a	n/a	n/a	n/a	Died at 22 mths secondary to HSV infection
P3	Y	N	N	N	Normal 5.26 (1.5-8)	Normal 46% (31-47)	Normal 36% (18-35)	Low-normal 239 (270-860)	Low 50 (100-480)	Normal 9.3 (5.4-16.1)	High-Normal 2.82 (0.7-2.5)	Low-Normal 0.46 (0.5-1.8)	Recurrent otitis media
P4	Y	Y	N	N	n/a	Normal 990 (600-1700)	Low 30 (400-1000)	Normal 170 (40-500)	Normal	n/a	n/a	n/a	IgM paraproteinaemia Affected sister died of respiratory infection
P5	Y	Y	Y	N	n/a	n/a	n/a	n/a	n/a	n/a	n/a	n/a	Poor response to vaccines. Recurrent pneumonia, urinary tract and upper respiratory tract infections. Chronic lung disease and bronchiectasis. Peripheral T cell lymphoma at 11yrs (large cell type)
P6	Y	Y Grp A strep	Y Influenza	N	Normal 5.38	n/a	n/a	n/a	n/a	n/a	n/a	n/a	

			RSV		(1.5-7.4)								
P7	N	N	N	N	n/a	n/a	n/a	n/a	n/a	n/a	n/a	n/a	
P8	Y	Y	Y Astrovirus EBV	N	Normal 5.64 (1.5-8.5)	Normal 1236 (850-1800)	Low 390 (650-1500)	Low-normal 552 (600-1300)	Low 98 (180-600)	Normal 6.73 (4-16)	Normal 2.97 (0.4-2)	Normal 0.64 (0.5-2)	Normal response to vaccine*
P9	Y	Y	Y Norovirus	N	Normal	Normal 1853 (850-1800)	Low 451 (650-1500)	Normal 1079 (600-1300)	High 1018 (180-600)	Normal 3.5 (3.1-13)	Normal 0.71 (0.3-1.2)	Low 0.31 (0.5-2.2)	Normal response to vaccine*
P10	N	N	N	N	Normal 2.8 (1.5-8)	Normal	Normal	Normal	Normal	1.8	4.3	1.7	
P11	Y	Klebseilla	N	N	n/a	n/a	n/a	n/a	n/a	n/a	n/a	n/a	Died at 3months with Klebsiella pneumonia.
P12	N	N	N	N	n/a	n/a	n/a	n/a	n/a	n/a	n/a	n/a	
P13	N	N	N	N	n/a	n/a	n/a	n/a	n/a	n/a	n/a	n/a	
P14	Y	Y MRSA	N	Y Candida	Normal 1.53 (1.0-8.53)	Low 753 (2815-6110)	Low 252 (394-1637)	Normal 991 (179-2657)	n/a	Low 1.5 (2.86-16.80)	Normal 0.11 (0.1-1.29)	Normal 0.25 (0.21-1.92)	Chronic cutaneous candidiasis & MRSA infection, T cell proliferative responses normal
P15	Y	N	Y	N	n/a	n/a	n/a	n/a	n/a	Normal	Low	Undetec-table	Chronic otitis media, nodular sclerosis Hodgkin's lymphoma at 28yrs

Table S4: Immunological Phenotype in POLE deficient individuals. Values included where available. Normal reference range for diagnostic lab where test performed in brackets. *Measured for Hib, Tetanus and Pneumococcus. n/a not available. BMT Bone Marrow Transplant.

Syndrome	Clinical Features	Gene(s)	Inheritance	Molecular mechanism	References
FILS	Facial Dysmorphism, Immunodeficiency, Livedo and Short Stature	*POLE* (2 families)	AR	Biallelic partial loss of function, homozygous splice mutation predicted to reduce levels of Polymerase Epsilon	Schmid *et al*, 2012[6], Thiffault *et al,* 2015[11]
IMAGe Syndrome	Intrauterine Growth Restriction, Metaphyseal dysplasia, Adrenal Insufficiency, Genitourinary abnormalties in males Plus variable immunodeficiency (POLE only)	*CDKN1C* *POLE*	AD (maternal allele only) AR	Imprinted gain of function mutations in PCNA binding domain. Biallelic loss of function mutations predicted to reduce levels of Polymerase Epsilon.	Arboleda *et al,* 2012[2] Current manuscript
MCM4 deficiency	Severe pre- and post-natal growth failure, Microcephaly, Immunodeficiency (decreased NK cells), Adrenal Insufficiency and cancer predisposition	*MCM4*	AR	Biallelic partial loss of function, homozygous splice mutations	Casey *et al*, 2012[12], Eidenschenk *et al*, 2006[13], Gineau *et al*, 2012[14], Hughes *et al*, 2012[15].
GINS1 deficiency	Intrauterine growth deficiency, Immunodeficiency (NK cell deficiency and chronic neutropenia), eczema	*GINS1*	AR	Biallelic partial loss of function mutations	Bernard *et al,* 2004[16], Cottineau *et al,* 2017[17]
Meier Gorlin	Microtia, Hypoplastic/Absent Patella, Short Stature Plus craniosynostosis (*CDC45* only)	*ORC1, ORC4, ORC6, CDT1, CDC6, CDC45* *GMNN*	AR AD	Biallelic partial loss of function mutations, impaired replication licencing *De novo* gain of function mutations	Bicknell *et al,* 2011[18; 19], Bongers *et al,* 2001[20], de Munnik *et al,* 2012[21], Fenwick *et al,* 2016[22] Burrage *et al,* 2015[23]
Rothmund-Thomson	Skin atrophy, telangiectasia, hyper-/hypo-pigmentation (poikiloderma congenitale), skeletal abnormalities, short stature, premature aging, cancer predisposition	*RECQL4*	AR	Biallelic loss and partial loss of function mutations	Kitao *et al,* 1999[24], Lindor *et al,* 2000[25], Wang *et al,* 2001[26]
Baller-Gerold	Craniosynostosis, radial aplasia, growth retardation, poikiloderma				Van Maldergem *et al*, 2006[27]
RAPADILINO	Radial and patella hypoplasia/aplasia, small stature, diarhhoea in infancy, dysmorphic features, cleft/high arched palate				Kaariainen *et al,* 1989[28], Siitonen *et al,* 2003[29]

Table S5: Summary of clinical and molecular genetic findings associated with disorders of the replisome. AR Autosomal Recessive, AD Autosomal Dominant.

Materials and Methods:

Research subjects

Genomic DNA was extracted from blood samples by standard methods or from saliva samples using Oragene collection kits according to the manufacturer's instructions. Informed consent was obtained from all participating families. The studies were approved by the ethics review boards, the Scottish Multicentre Research Ethics Committee (05/MRE00/74) and the University of Texas Southwestern Medical Center. Parents provided written consent for the publication of photographs of the affected individuals.

Whole-Genome Sequencing, Whole-Exome Sequencing and Analysis

Whole Genome Sequencing in P1, P3 and P4 was performed by Edinburgh Genomics (Clinical Division) as part of the Scottish Genomes Project (SGP) to 30X coverage using TruSeq Nano library preparation kits and a HiSeq X sequencing platform (Illumina). FASTQs generated by Edinburgh Genomics were aligned to the human genome (hg38, including alt, decoy and HLA sequences) using bwa mem[30] (0.7.13). Post-processing was performed with samblaster[31] (0.1.22) to mark duplicate reads, and the Genome Analysis ToolKit[32] (GATK, v3.4-0-g7e26428) for indel realignment and base recalibration. Genotype likelihoods for each sample were calculated using the GATK HaplotypeCaller and resulting GVCF files were called jointly using GATK's GenotypeGVCFs function. Variant quality score recalibration (VQSR) was performed as per GATK best-practices[33] and a truth sensitivity threshold of 99.9% applied.

Functional annotations were added using Ensembl's Variant Effect Predictor[34] (v84). VASE (v0.1, https://github.com/gantzgraf/vase) was used to perform variant filtering and burden analysis. Variants were filtered to remove those outside the 99.9% truth sensitivity threshold from VQSR, with a frequency greater than 0.1% in gnomAD or dbSNP147, or in segmentally duplicated regions or regions of low sequence complexity. Allele counts were generated for genotype calls with a minimum PHRED scale genotype quality score of 20 for each canonical transcript in the GENCODE basic transcript set where the alternative allele resulted in predicted loss of function (stop gain, stop loss, splice donor/acceptor site disruption or indels resulting in frameshifts). Allele counts per transcript were compared with variant data from gnomAD[35].

WGS in P10-14 was performed by the Hudson Alpha Genome sequencing Centre to an average 40X coverage using a HiSeq platform (Illumina) and analysed using DRAGEN software (Edico Genome). Whole Exome Sequencing in P5 and P6 was performed as described previously[36]. WES in P15 was performed as previously described[37; 38].

All *POLE* variants identified were confirmed by capillary sequencing, using standard methodology. Details of primers listed below.

Haplotype Analysis

Variants surrounding rs762985435 were identified from WGS and WES VCF files and analysed for shared haplotypes in samples with this SNP using bespoke software (available at https://github.com/gantzgraf/het_hap_phaser).

Cell Culture

Primary dermal fibroblasts (Patient P2, P3) were established from skin punch biopsies in AmnioMax medium (Life Technologies) and then maintained in Dulbecco's MEM (modified Eagle's medium; DMEM) supplemented with 10% fetal bovine serum, 5% L-glutamine and 5% penicillin/streptomycin, at 5% CO_2 and 3% O_2. Patient 1 primary fibroblasts were a kind gift from Prof. Penny Jeggo, University of Sussex. Genotypes of patient cell lines were validated by Sanger sequencing and immunoblotting.

RT-PCR

Total RNA was extracted from cell lines using the RNeasy kit (Qiagen) according to the manufacturer's instructions. Following DNase I (Qiagen) treatment cDNA was generated using SuperScript III Reverse Transcriptase kit (Thermo Fisher Scientific). RT-PCR was performed on cDNA using primers in exon 14 and 17 (details below).

Mini-Gene Assay

A 1.6 kb stretch of the *POLE* gene encompassing the 3' end of intron 12, exon 13, intron 13, exon 14, intron 14, exon 15, intron 15, exon 16 and the 5' end of intron 16 was amplified using DNA from control genomic DNA with SalI-pole-int12-F and XbaI-pole-int16-R primers, and cloned into the RHCglo vector[39] using SalI and XbaI restriction sites. Site-directed mutagenesis was used to introduce the *POLE* intron 15 patient mutation c.1686+32C>G and as a positive control, *POLE* intron 15 splice donor mutation (c.1686+1G>A) into the splicing reporter construct. HeLa cells were transfected with each individual splicing mutation reporter construct using Lipofectamine 2000 according the manufacturer's instructions. Twenty-four hours after transfection, cells were harvested, total cellular RNA extracted, and cDNA generated using Superscript III reverse transcriptase first-stand synthesis system (Invitrogen). PCR was carried out using primers (RSV5U-minigene-F and RTRHC-minigene-R) to the 5' and 3' ends of the artificial exons present in the RHCglo vector. cDNA amplicons for WT and mutated *POLE* were resolved on a 2% agarose gel to visualize differences in splicing. Individual PCR products were subsequently cloned into the pGEM-T Easy Vector (Promega) and sequenced to verify the exon content of each transcript. All relevant primers details are listed below.

Western blot analysis and antibodies

Whole cell extracts were obtained by lysis and sonication of cells in UTB buffer (8 M Urea, 50 mM Tris pH 7.5, 150 mM β-mercaptoethanol, protease inhibitor cocktail (Roche)) or in NP-40 lysis buffer 23(50 mM Tris pH 8.0, 280 mM NaCl, 0.5% NP-40, 0.2 mM EDTA, 0.2 mM EGTA, 10% Glycerol, 1 mM DTT, protease inhibitor cocktail (Roche), 1 mM PMSF, phosphatase inhibitors (40 mM NaF, 1 mM sodium orthovanadate)) and analyzed by SDS-PAGE following standard procedures. Protein samples were run on 6-12% acrylamide SDS-PAGE or 4-12% NuPage mini-gels (Life Technologies) and transferred onto nitrocellulose membrane. Immunoblotting was performed using antibodies to POLE (93H3A clone; Thermofisher Scientific cat# MA5-13616 at 2 µg/ml) and Vinculin (2C6-1B5 clone; Novusbio cat# H00007414-M01 1/5,000 dilution) (Figure S6). Chromatin fractionation experiments were performed as described in Bellelli *et al*., 2014[40], immunoblotting with POLE antibody, GTX132100, GeneTex.

FACS analysis

Non-confluent, primary fibroblasts grown in AmnioMax medium (Life Technologies) were pulse labeled with 10 µM BrdU for 30 min, washed and then harvested at 0, 4 and 8 h time points before fixation with 70% ethanol at -20°C for 16 h. Fixed cells were then digested with 1 mg/ml pepsin, denatured in 2 M HCl, and washed with PBS. After blocking in 0.5% BSA, 0.5% Tween-20, BrdU labelling was detected using anti-BrdU antibody (Abcam, ab6326; 1:75) and FITC-conjugated anti-rat secondary antibody, and DNA content determined by co-staining with 50 µg/ml propidium iodide. Cells were sorted on a BD Biosciences FACS Aria II and data analyzed using FlowJo software (v7.6.1, Tree Star) (Figure S7).

Code Availability

All custom code used in this study available at github.com (https://github.com/gantzgraf/vase and https://github.com/gantzgraf/het_hap_phaser) licensed under the MIT free software license.

Primer sequences for screening of *POLE* exons and flanking sequences

Exon	Forward Primer Sequence 5'-3'	Reverse Primer Sequence 5'-3'
1	ATTTCCGGCTCTCGCGAG	CCCTACCCCAGTCAGGCG
2	TGTCGCCTGTGGTCCCAG	CTCATGTGTCCCCCACTCTT
3	AGTGCTGAGTTTCCCGAAAG	CCTCCCTGACAGTCACAGAG
4	GGAGCAAGCAATGTGTTTTCA	GCTCACAACCCTAATCAGGATC
5	CTGTGGTGGGCTTTGCAAC	GATCCCACCTGCCAGGAA
6	GTGCAGAGTTGGACAAGGTG	ACAGAGCCAGCCATTAAGGT
7	TCCTCGGTTTGAACTCTGGT	CCTGCAAAACACACAGTGTG
8	GCCTCTCCATTGACCTGAAG	TTTGGGGGAAAAGCAGCAAA
9	AGAGGGAGGTAGAGCAGGC	AACAGTGGGGCAGATGCT
10	TAGGCAGAGTGTGTGGGC	GCCTGAGGCCTTGGAAAGAT
11	ACTTTGGGAGAGGAATTTGGAA	CTAAGTCGACATGGGAAGCG
12	GGGAGGAATGGAGAAAGGGG	GATGTGGTGACAGCACAGTC
13	GTTTTGCCAGTTCTCAGGGG	AGGACAAAACACGTGTGTCC
14	CAGGCTTTGCTTTCTGTGCT	CAGCTCCAGTGCATTTGGAA
15	TAGGTTCCTGGACTTTGCCT	TGGGACAGGATGGGGAGA
16	GAGCTTTCTCGGGCACAAC	CTGCTGAAAGACGTGGTCTG
17	AAAAGGGGTTGGTGAACTGC	TTCGTCCACCATGGCAGAG
18	GCCTGCAGGTGAGACTTTAC	CAAAAGGAGGCACAGACACA
19	GGGCGAGTTCAGTGAGTGT	CCAGCTGGGATGGACCAA
20	ATGTTCTTCAGCACCCCTGT	AGTGCCCACTTCATGAGCC
21	TGTACACTCTTCATTGTACTGGT	TGAATCAGATGAACGGCCCT
22	CCTCCTCCCTACTCCTCACT	TTCCTTCCTGCCCAGTGTG
23	GAAGGAGGGAAGGCTGGAG	TGCAGAGCCAGTGACATCAG
24	TGTGGAAAAGCCTCGGTTTG	ATCCTGGCTCCTGATCCAAC
25	AGAGGATGAGGCACAGCTG	TGTTCTTCGGTCACCTTGGT
26	CTAGAGGAGCACAGTCCAGG	TGGACACTTATGCCATCCCC
27	CGTCCTTATTTCCATGTTCATTTGA	AGTGAAGACGCCAGACAAAA
28	CCTGTGCTCAGCATGAAGTG	AGGCCAACACCCATCAGAG
29	GCGCCATCCAGAAGATCATC	CACTACAGCACACACAGCAG
30	CAATTCTCCTGTCTTGGCCT	CTCCCTAGGGGTCAGGAC
31	GGAGGCTGCTTGTGAGAAAG	CTCCCATCCCAGACCTCAG
32	CATCGTAGGGAGGCCTAAGG	TCACACACGTTGTTTTGAGGA
33	AGGACTCCGAATAGCGTGTG	GACTTCTGCCCGGGATGT
34	ATCCCGGGCAGAAGTCAC	GCGGATACTCCCTGGAGAAG
35	AGTTCAGCTACCTGGAACCA	GGACAAGACCTGGAGGGC
36	CTTTGCCCATGAGTGCTTGT	CCTGGGTCAAGGCAAAATGG
37	GCTGTGTGAGCCCCATCTT	CACCAGGGCACAGGTCAG
38	TACTGTCGTTGTGGGCCAG	TGCCTTGAGAAGATGTCACAG
39	CTGGTTCTGGAGGTGGTGG	GCCCAATGGACCCTGTCTTA
40	GGGAAAACCTGTGCCCATTT	CATGTCTCTGGTTCTGGGGA
41	ACCCTCAGCTCTTTTCCCTC	GCTGCTCAGATTCACCATGG
42	ACAAGGGGAAATAAAGGAAAGTTG	CACACTGACGTGCTTGTCTG
43	AGGAAGGCCTCTGGTCAAAC	GATACCATGGCACAGGAGC
44	TCTGTGAGGCAATCTGACCA	ATAAGGATGCTGAGGGAGGG
45	GTGCCAGTGACCTAACTCCT	TACAGCCTCACCTTGCACA
46	GTTCTGGTCCAGACAGAGCA	ATCCATGTGAGTCAGAGGGG
47	ACCAGGCGCTTCTCACAG	CCCCTTGGAAGACACCAGG

Exon	Forward Primer Sequence 5'-3'	Reverse Primer Sequence 5'-3'
48	GGGATGAGGTCGTGCATTTT	TAGTGCTGGGCAATGTTCCG
49	CTCTCCCTCATCTGCCTCG	AGTGGTCTGGTCACTGGAAG

RT PCR primer sequences

RT PCR primers	sequence 5'-3'
RT PCR primer F	TCTGGCCACGTATTCTGTGT
RT PCR primer R	CTTCAGGGAGGCAAGCTTG

Primers used for minigene assay cloning, mutagenesis and PCR

Primer	sequence 5'-3'
SalI-pole-int12-F	TCTAGTCGACCTGCATGTTAGAATCATCCTG
XbaI-pole-int16-R	CTAGTCTAGAGTGGTCTGTGAAGAAGGCG
pole-c.1686+32C>G F	CTGGGATTCAGATTCTTCGCACTCTTGTGCTGTG
pole-c.1686+32C>G R	CACAGCACAAGAGTGCGAAGAATCTGAATCCCAG
pole-c.1686+1G>A F	CCCTTGCCGGTTTAGGATGATGTGCTTCTTCC
pole-c.1686+1G>A R	GGAAGAAGCACATCATCCTAAACCGGCAAGGG
RSV5U-minigene-F	CATTCACCACATTGGTGTGC
RTRHC-minigene-R	GGGCTTTGCAGCAACAGTAAC

Antibodies used in experimental procedures

Antibody	Antibody species	Application	Manufacturer	Catalogue Number
Anti-POLE Monoclonal Antibody (93H3A)	Mouse	WB	Thermo Fisher	MA5-13616
Anti-Vinculin Antibody (2C6-1B5)	Mouse	WB	Novus Biologicals	H00007414-M01
Monoclonal Anti-α-Tubulin Antibody	Mouse	WB	Sigma-Aldrich	T9026
Anti-Histone H3 antibody	Mouse	WB	Abcam	ab10799
Anti-POLE antibody	Rabbit	WB	GeneTex	GTX132100
Anti-BrdU antibody	Rat	FACS	Abcam	ab6326

References

1. Vilain, E., Le Merrer, M., Lecointre, C., Desangles, F., Kay, M.A., Maroteaux, P., and McCabe, E.R. (1999). IMAGe, a new clinical association of intrauterine growth retardation, metaphyseal dysplasia, adrenal hypoplasia congenita, and genital anomalies. J Clin Endocrinol Metab 84, 4335-4340.
2. Arboleda, V.A., Lee, H., Parnaik, R., Fleming, A., Banerjee, A., Ferraz-de-Souza, B., Delot, E.C., Rodriguez-Fernandez, I.A., Braslavsky, D., Bergada, I., et al. (2012). Mutations in the PCNA-binding domain of CDKN1C cause IMAGe syndrome. Nat Genet 44, 788-792.
3. Bennett, J., Schrier Vergano, S.A., and Deardorff, M.A. (1993). IMAGe Syndrome. In GeneReviews((R)), M.P. Adam, H.H. Ardinger, R.A. Pagon, S.E. Wallace, L.J.H. Bean, K. Stephens, andA. Amemiya, eds. (Seattle (WA).
4. Pedreira, C.C., Savarirayan, R., and Zacharin, M.R. (2004). IMAGe syndrome: a complex disorder affecting growth, adrenal and gonadal function, and skeletal development. J Pediatr 144, 274-277.
5. Tan, T.Y., Jameson, J.L., Campbell, P.E., Ekert, P.G., Zacharin, M., and Savarirayan, R. (2006). Two sisters with IMAGe syndrome: cytomegalic adrenal histopathology, support for autosomal recessive inheritance and literature review. Am J Med Genet A 140, 1778-1784.
6. Pachlopnik Schmid, J., Lemoine, R., Nehme, N., Cormier-Daire, V., Revy, P., Debeurme, F., Debre, M., Nitschke, P., Bole-Feysot, C., Legeai-Mallet, L., et al. (2012). Polymerase epsilon1 mutation in a human syndrome with facial dysmorphism, immunodeficiency, livedo, and short stature ("FILS syndrome"). J Exp Med 209, 2323-2330.
7. Hamajima, N., Johmura, Y., Suzuki, S., Nakanishi, M., and Saitoh, S. (2013). Increased protein stability of CDKN1C causes a gain-of-function phenotype in patients with IMAGe syndrome. PLoS One 8, e75137.
8. Borges, K.S., Arboleda, V.A., and Vilain, E. (2015). Mutations in the PCNA-binding site of CDKN1C inhibit cell proliferation by impairing the entry into S phase. Cell Div 10, 2.
9. Furstenthal, L., Swanson, C., Kaiser, B.K., Eldridge, A.G., and Jackson, P.K. (2001). Triggering ubiquitination of a CDK inhibitor at origins of DNA replication. Nat Cell Biol 3, 715-722.
10. Chuang, L.C., and Yew, P.R. (2005). Proliferating cell nuclear antigen recruits cyclin-dependent kinase inhibitor Xic1 to DNA and couples its proteolysis to DNA polymerase switching. J Biol Chem 280, 35299-35309.
11. Thiffault, I., Saunders, C., Jenkins, J., Raje, N., Canty, K., Sharma, M., Grote, L., Welsh, H.I., Farrow, E., Twist, G., et al. (2015). A patient with polymerase E1 deficiency (POLE1): clinical features and overlap with DNA breakage/instability syndromes. BMC Med Genet 16, 31.
12. Casey, J.P., Nobbs, M., McGettigan, P., Lynch, S., and Ennis, S. (2012). Recessive mutations in MCM4/PRKDC cause a novel syndrome involving a primary immunodeficiency and a disorder of DNA repair. J Med Genet 49, 242-245.
13. Eidenschenk, C., Jouanguy, E., Alcais, A., Mention, J.J., Pasquier, B., Fleckenstein, I.M., Puel, A., Gineau, L., Carel, J.C., Vivier, E., et al. (2006). Familial NK cell deficiency associated with impaired IL-2- and IL-15-dependent survival of lymphocytes. J Immunol 177, 8835-8843.
14. Gineau, L., Cognet, C., Kara, N., Lach, F.P., Dunne, J., Veturi, U., Picard, C., Trouillet, C., Eidenschenk, C., Aoufouchi, S., et al. (2012). Partial MCM4 deficiency in patients with growth retardation, adrenal insufficiency, and natural killer cell deficiency. J Clin Invest 122, 821-832.
15. Hughes, C.R., Guasti, L., Meimaridou, E., Chuang, C.H., Schimenti, J.C., King, P.J., Costigan, C., Clark, A.J., and Metherell, L.A. (2012). MCM4 mutation causes adrenal failure, short stature, and natural killer cell deficiency in humans. J Clin Invest 122, 814-820.
16. Bernard, F., Picard, C., Cormier-Daire, V., Eidenschenk, C., Pinto, G., Bustamante, J.C., Jouanguy, E., Teillac-Hamel, D., Colomb, V., Funck-Brentano, I., et al. (2004). A novel developmental and immunodeficiency syndrome associated with intrauterine growth retardation and a lack of natural killer cells. Pediatrics 113, 136-141.

17. Cottineau, J., Kottemann, M.C., Lach, F.P., Kang, Y.H., Vely, F., Deenick, E.K., Lazarov, T., Gineau, L., Wang, Y., Farina, A., et al. (2017). Inherited GINS1 deficiency underlies growth retardation along with neutropenia and NK cell deficiency. J Clin Invest 127, 1991-2006.
18. Bicknell, L.S., Bongers, E.M., Leitch, A., Brown, S., Schoots, J., Harley, M.E., Aftimos, S., Al-Aama, J.Y., Bober, M., Brown, P.A., et al. (2011). Mutations in the pre-replication complex cause Meier-Gorlin syndrome. Nat Genet 43, 356-359.
19. Bicknell, L.S., Walker, S., Klingseisen, A., Stiff, T., Leitch, A., Kerzendorfer, C., Martin, C.A., Yeyati, P., Al Sanna, N., Bober, M., et al. (2011). Mutations in ORC1, encoding the largest subunit of the origin recognition complex, cause microcephalic primordial dwarfism resembling Meier-Gorlin syndrome. Nat Genet 43, 350-355.
20. Bongers, E.M., Opitz, J.M., Fryer, A., Sarda, P., Hennekam, R.C., Hall, B.D., Superneau, D.W., Harbison, M., Poss, A., van Bokhoven, H., et al. (2001). Meier-Gorlin syndrome: report of eight additional cases and review. Am J Med Genet 102, 115-124.
21. de Munnik, S.A., Bicknell, L.S., Aftimos, S., Al-Aama, J.Y., van Bever, Y., Bober, M.B., Clayton-Smith, J., Edrees, A.Y., Feingold, M., Fryer, A., et al. (2012). Meier-Gorlin syndrome genotype-phenotype studies: 35 individuals with pre-replication complex gene mutations and 10 without molecular diagnosis. Eur J Hum Genet 20, 598-606.
22. Fenwick, A.L., Kliszczak, M., Cooper, F., Murray, J., Sanchez-Pulido, L., Twigg, S.R.F., Goriely, A., McGowan, S.J., Miller, K.A., Taylor, I.B., et al. (2016). Mutations in CDC45, Encoding an Essential Component of the Pre-initiation Complex, Cause Meier-Gorlin Syndrome and Craniosynostosis. American Journal of Human Genetics.
23. Burrage, L.C., Charng, W.L., Eldomery, M.K., Willer, J.R., Davis, E.E., Lugtenberg, D., Zhu, W., Leduc, M.S., Akdemir, Z.C., Azamian, M., et al. (2015). De Novo GMNN Mutations Cause Autosomal-Dominant Primordial Dwarfism Associated with Meier-Gorlin Syndrome. Am J Hum Genet 97, 904-913.
24. Kitao, S., Shimamoto, A., Goto, M., Miller, R.W., Smithson, W.A., Lindor, N.M., and Furuichi, Y. (1999). Mutations in RECQL4 cause a subset of cases of Rothmund-Thomson syndrome. Nat Genet 22, 82-84.
25. Lindor, N.M., Furuichi, Y., Kitao, S., Shimamoto, A., Arndt, C., and Jalal, S. (2000). Rothmund-Thomson syndrome due to RECQ4 helicase mutations: report and clinical and molecular comparisons with Bloom syndrome and Werner syndrome. Am J Med Genet 90, 223-228.
26. Wang, L.L., Levy, M.L., Lewis, R.A., Chintagumpala, M.M., Lev, D., Rogers, M., and Plon, S.E. (2001). Clinical manifestations in a cohort of 41 Rothmund-Thomson syndrome patients. Am J Med Genet 102, 11-17.
27. Van Maldergem, L., Siitonen, H.A., Jalkh, N., Chouery, E., De Roy, M., Delague, V., Muenke, M., Jabs, E.W., Cai, J., Wang, L.L., et al. (2006). Revisiting the craniosynostosis-radial ray hypoplasia association: Baller-Gerold syndrome caused by mutations in the RECQL4 gene. J Med Genet 43, 148-152.
28. Kaariainen, H., Ryoppy, S., and Norio, R. (1989). RAPADILINO syndrome with radial and patellar aplasia/hypoplasia as main manifestations. Am J Med Genet 33, 346-351.
29. Siitonen, H.A., Sotkasiira, J., Biervliet, M., Benmansour, A., Capri, Y., Cormier-Daire, V., Crandall, B., Hannula-Jouppi, K., Hennekam, R., Herzog, D., et al. (2009). The mutation spectrum in RECQL4 diseases. Eur J Hum Genet 17, 151-158.
30. Li, H. (2013). Aligning sequence reads,clone sequences and assembly contigs with BWA-MEM.
31. Faust, G.G., and Hall, I.M. (2014). SAMBLASTER: fast duplicate marking and structural variant read extraction. Bioinformatics 30, 2503-2505.
32. McKenna, A., Hanna, M., Banks, E., Sivachenko, A., Cibulskis, K., Kernytsky, A., Garimella, K., Altshuler, D., Gabriel, S., Daly, M., et al. (2010). The Genome Analysis Toolkit: a MapReduce framework for analyzing next-generation DNA sequencing data. Genome Res 20, 1297-1303.

33. Van der Auwera, G.A., Carneiro, M.O., Hartl, C., Poplin, R., Del Angel, G., Levy-Moonshine, A., Jordan, T., Shakir, K., Roazen, D., Thibault, J., et al. (2013). From FastQ data to high confidence variant calls: the Genome Analysis Toolkit best practices pipeline. Curr Protoc Bioinformatics 43, 11 10 11-33.
34. McLaren, W., Gil, L., Hunt, S.E., Riat, H.S., Ritchie, G.R., Thormann, A., Flicek, P., and Cunningham, F. (2016). The Ensembl Variant Effect Predictor. Genome Biol 17, 122.
35. Lek, M., Karczewski, K.J., Minikel, E.V., Samocha, K.E., Banks, E., Fennell, T., O'Donnell-Luria, A.H., Ware, J.S., Hill, A.J., Cummings, B.B., et al. (2016). Analysis of protein-coding genetic variation in 60,706 humans. Nature 536, 285-291.
36. Martin, C.A., Ahmad, I., Klingseisen, A., Hussain, M.S., Bicknell, L.S., Leitch, A., Nurnberg, G., Toliat, M.R., Murray, J.E., Hunt, D., et al. (2014). Mutations in PLK4, encoding a master regulator of centriole biogenesis, cause microcephaly, growth failure and retinopathy. Nat Genet 46, 1283-1292.
37. Yang, Y., Muzny, D.M., Reid, J.G., Bainbridge, M.N., Willis, A., Ward, P.A., Braxton, A., Beuten, J., Xia, F., Niu, Z., et al. (2013). Clinical whole-exome sequencing for the diagnosis of mendelian disorders. N Engl J Med 369, 1502-1511.
38. Yang, Y., Muzny, D.M., Xia, F., Niu, Z., Person, R., Ding, Y., Ward, P., Braxton, A., Wang, M., Buhay, C., et al. (2014). Molecular findings among patients referred for clinical whole-exome sequencing. JAMA 312, 1870-1879.
39. Singh, G., and Cooper, T.A. (2006). Minigene reporter for identification and analysis of cis elements and trans factors affecting pre-mRNA splicing. Biotechniques 41, 177-181.
40. Bellelli, R., Castellone, M.D., Guida, T., Limongello, R., Dathan, N.A., Merolla, F., Cirafici, A.M., Affuso, A., Masai, H., Costanzo, V., et al. (2014). NCOA4 transcriptional coactivator inhibits activation of DNA replication origins. Mol Cell 55, 123-137.